J|A|C|S
COMMUNICATIONS

Published on Web 09/06/2003

# Mimicking Photosynthesis in a Computationally Designed Synthetic Metalloprotein

Lidia Cristian, Piotr Piotrowiak, and Ramy S. Farid*

*Department of Chemistry, Rutgers, The State University of New Jersey, 73 Warren Street, Newark, New Jersey 07102*

Received November 4, 2002; E-mail: rfarid@newark.rutgers.edu

The construction of efficient solar energy converting systems has been the subject of extensive research in the past decades. For example, important progress has been made toward the design and construction of chemical assemblies that function as artificial reaction centers (RC).[1] While advances in protein design have made possible the construction of protein architectures with nativelike properties and predictable structures[2] and function,[3] there are as of yet no examples of functional protein-based solar energy conversion systems. We believe the lack of functional protein-based RCs is primarily due to the difficulty associated with designing and constructing stable, well-structured frameworks upon which efficient systems can be built. This communication describes the design and characterization of an artificial RC protein that closely resembles the function of the natural photosynthetic reaction center: the synthetic protein participates in multiple reduction/oxidation cycles with exogenous acceptors/donors following photoexcitation.

We previously constructed an electron-transfer protein that efficiently converts light into chemical energy, that was built by engineering the parameters that govern protein-mediated electron-transfer rates: distance ($R$), driving force ($\Delta G$) and reorganization energy ($\lambda$).[4] We extend here this strategy to the construction of an artificial RC protein, designed with the use of *CORE*, a protein design program developed in our group.[5] The designed metalloprotein (aRC) consists of a tetrahelical bundle functionalized with two bis-histidine-bound metal cofactors: a $Ru(bpy)_2$ moiety and a heme group. The tetrahelical scaffold is comprised of two identical 54-residue helix−loop−helix [HLH] peptides joined through a disulfide bond between the C-terminal cysteines to yield an antiparallel four-helix bundle. Two bis-histidine binding sites at positions 21 and 42 were engineered for $Ru(bpy)_2$ and heme binding, respectively (Figure 1).

Positioning of the hydrophilic and hydrophobic residues was guided by the $a-r$ method, described elsewhere.[6] The hydrophilic exterior of the helices was designed to stabilize the bundle primarily through salt bridges between Glu and Lys. The identity of the hydrophobic core residues was determined using *CORE*, which optimizes the heat capacity of unfolding ($\Delta C_p$) and the side chain entropy ($\Delta S_{conf}$), parameters that are correlated to protein thermal stability and cooperativity, respectively. The input into *CORE* was the backbone structure shown in Figure 1 in which all core positions were initially set to Ala and the bound cofactors and exterior hydrophilic residues are held fixed. The sequence[7] output by *CORE* that corresponded to the largest value for $\Delta C_p$ and lowest value for $\Delta S_{conf}$ was synthesized using standard automated solid-phase peptide synthesis to produce the helix−loop−helix peptide.[8] Incorporation of the $Ru(bpy)_2$ group into $[HLH]_2$ was achieved by reaction with $Ru(bpy)_2CO_3$.[4] The location of the bound ruthenium complex at the designed site was confirmed by chemical cleavage with cyanogen bromide (CNBr) at the Met residue located in the loop between helices followed by MALDI-TOF MS analysis.[9]

The absorption and emission spectra of the ruthenium-modified protein, $Ru[HLH]_2$, are consistent with bis-histidine ligation (see Supporting Information). The lifetime of the triplet exited state of $Ru[HLH]_2$ was determined to be $150 \pm 10$ ns.[10]

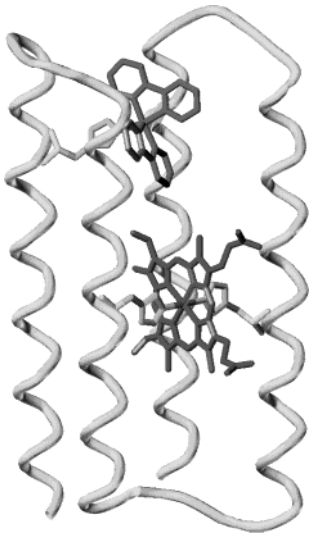

***Figure 1.*** Model structure of the designed protein, aRC, with $Ru(bpy)_2$ chelated to His21 pair (top) and heme bound to His42 pair (middle).

The CD spectra of $[HLH]_2$ and $Ru[HLH]_2$ reveal $80 \pm 5\%$ α−helical content for both proteins (see Supporting Information). CD spectroscopy was also employed to confirm that, as designed, cis-Λ-$[Ru(bpy)_2(his)_2]$ isomer binds to the protein scaffold. The CD spectrum from 265 to 450 nm of the Ru-modified protein shows the same signature bands as that of the reference molecule, cis-Λ-$[(Ru(bpy)_2(H_2O)(py)](ClO_4)_2$ (see Supporting Information).[11]

The ruthenium-modified protein binds hemin tightly with a $K_d = 35 \pm 30$ nM. The absorption features of the bound heme (see Supporting Information) are remarkably similar to those of native bis-histidine-ligated *b*-type cytochromes, indicating that heme binds to $Ru[HLH]_2$ via bis-histidine ligation in a unique, well-defined environment.

The reduction potential for heme in aRC was determined to be $-115 \pm 10$ mV vs NHE using the spectroelectrochemical procedure described elsewhere.[6] This value is more positive than most other synthetic hemoproteins with bis-histidine-bound heme groups. This suggests a more effective shielding of the heme group from water, consistent with the observed tight heme binding. The redox potential for $Ru[HLH]_2$ was estimated to be +1.25 V based on the potential of the model compound $Ru(bpy)_2im_2$ in DMF.

Photoexcitation of aRC leads to efficient quenching of the luminescence of the ruthenium complex by the heme group. A lower limit of $5 \times 10^{10}$ $s^{-1}$ was estimated for the intramolecular photoinduced forward ET rate constant from steady-state luminescence measurements. The charge recombination process, monitored by transient absorption spectroscopy,[12] follows first-order kinetics yielding a back-electron transfer, $k_b = 1.4 \times 10^7$ $s^{-1}$ (see Supporting Information). These results indicate that upon excitation of aRC,



10.1021/ja0292142 CCC: $25.00 

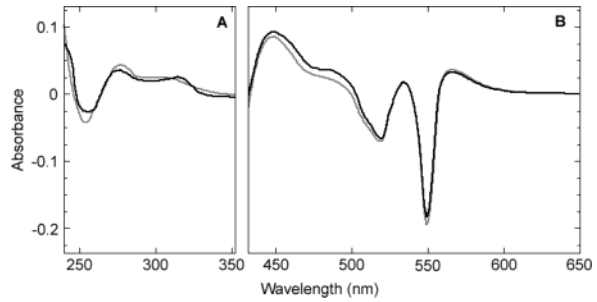


***Figure 2.*** Light minus dark difference spectrum obtained by irradiating 1 $\mu$M aRC in the presence of 20 $\mu$M reduced cytochrome *c* (exogenous donor) and 20 $\mu$M naphthoquinone-2-sulfonate (exogenous acceptor).[14] (A) Black: experimental light minus dark spectrum minus authentic 10 $\mu$M oxidized minus reduced cyt *c*. Gray: authentic 10 $\mu$M reduced minus neutral naphthoquinone-2-sulfonate. (B) Black: experimental light minus dark spectrum. Gray: authentic oxidized minus reduced 10 $\mu$M cyt *c*. See Supporting Information for experimental details.

rapid photoinduced ET from $Ru(bpy)_2$ to heme occurs, followed by an approximately 3 orders of magnitude slower charge recombination step, yielding a charge-separated state (CSS) with a lifetime of 70 ns. The most likely explanation for this is a low reorganization energy ($\lambda = 0.5$ eV) which gives rise to a relatively steep Marcus inverted region.[13]

This long-lived CSS makes feasible coupling aRC with an exogenous donor and acceptor to convert the stored electrical energy into chemical redox energy, thus mimicking the basic function of the natural photosynthetic RC. Indeed, conversion of light into chemical energy is observed upon photoexcitation of aRC in the presence of two exogenous redox molecules of the type present in natural bacterial photosynthesis. Cytochrome *c* (cyt *c*) was chosen as the electron donor and naphthoquinone-2-sulfonate as the electron acceptor for their electrochemical properties and solubility in aqueous media.[14] Figure 2 shows that photoexcitation of aRC in the presence of excess reduced cyt *c* and naphthoquinone-2-sulfonate results in multiple turnovers whereby cyt *c* is oxidized and the quinone is reduced. These results are consistent with the following sequence of reactions: Photoexcitation of the aRC−cyt *c*−quinone system results in the formation of the excited state, $*Ru^{II}-Fe^{III}$, followed by fast intramolecular ET from $*Ru^{II}$ to heme to produce the $Ru^{III}-Fe^{II}$ CSS. This is followed by two independent bimolecular ET reactions: (1) one in which the photogenerated $Fe^{II}$ reduces the naphthoquinone acceptor (Q) to yield the corresponding semiquinone radical anion, $Q^{-\bullet}$, which is rapidly protonated to form the neutral semiquinone radical, $QH^{\bullet}$; (2) the other in which the photogenerated $Ru^{III}$ species oxidizes cyt *c*. In the net reaction, visible light is converted into chemical redox energy in the form of the products, cyt $c^+$ and $QH^{\bullet}$. Moreover, the spectrum in Figure 2 demonstrates that this occurs for at least 10 photocycles.

It should be noted that the two thermal ET processes (reduction of Q and oxidation of cyt *c*) are exothermic reactions and kinetically controlled. No attempt was made to probe or influence the sequence of these reactions; however, being bimolecular, the rates can obviously be controlled by varying the reactant concentrations.

A number of control experiments were carried out to rule out other reactions that might lead to the observed products. Irradiation of Q and cyt *c* yielded no reactions as did irradiation of the ruthenium-modified protein ($Ru[HLH]_2$) and Q. In addition, irradiation of aRC in the presence of Q without adding cyt *c* yields just one equivalent of $QH^{\bullet}$. Similarly, irradiation of aRC in the presence of cyt *c* without adding Q yields just one equivalent of cyt $c^+$.

These control experiments clearly show that three ET reactions must occur to produce the reduced Q and oxidized cyt *c* products. The first is photoinduced ET from the excited ruthenium complex [*Ru(II)] to oxidized heme [Fe(III)] followed by reduction of the quinone by the reduced heme [Fe(II)] and oxidation of the cyt *c* by oxidized ruthenium [Ru(III)].

Through a combination of automated computational protein design and knowledge of the engineering principles of biological electron tunneling extracted from natural electron-transfer systems, it was possible to construct a system that functions much like native photosynthetic RCs. Donor/acceptor distance, free energy, and reorganization energy were optimized to allow efficient charge separation and slow charge recombination. Although protein complexes that mimic some of the steps of native RCs have been reported,[15] the present system represents the first example of a functional protein-based artificial RC.

**Supporting Information Available:** Absorption, emission and CD spectra of $Ru[HLH]_2$, and transient absorption spectrum of aRC (PDF). This material is available via the Internet at http://pubs.acs.org.

## References

(1) (a) Steinberg-Yfrach, G.; Liddell, P.; Hung, S.; Moore, A.; Gust, D.; Moore, T. *Nature* **1997**, *385*, 239. (b) Steinberg-Yfrach, G.; Rigaud, J. L.; Durantini, E. N.; Moore, A. L.; Gust, D.; Moore, T. A. *Nature* **1998**, *392*, 479. (c) Wasielewski, M. R. *Chem. Rev.* **1992**, *92*, 435.

(2) (a) Hill, B. R.; Raleigh, D. P.; Lombardi, A.; DeGrado, W. F. *Acc. Chem. Res.* **2000**, *33*, 745. (b) DeGrado, W. F.; Summa, C. M.; Pavone, V.; Nastri, F.; Lombardi, A. *Annu. Rev. Biochem.* **1999**, *68*, 779. (c) Hill, B. R.; DeGrado, W. F. *J. Am. Chem. Soc.* **1998**, *120*, 1138.

(3) (a) Mutz, M. W.; Case, M. A.; Wishart, J. F.; Ghadiri, M. R.; McLendon, G. L. *J. Am. Chem. Soc.* **1999**, *121*, 858 (b) Rau, H. K.; DeJonge, N.; Haehnel, W. *Proc. Natl. Acad. Sci. U.S.A.* **1998**, *95*, 11526.

(4) Cristian, L. Ph.D. Thesis, Rutgers, The State University of New Jersey, Newark, NJ, 2002.

(5) Jiang, X.; Farid, H.; Pistor, E.; Farid, R. S. *Protein Sci.* **2000**, *9*, 403.

(6) Xu, Z.; Farid, R. S. *Protein Sci.* **2001**, *10*, 236−249.

(7) $NH_2$-NKWEEIWKEAAKKLEEFIKKHEEAAKGMGNAKKWAEKA-KEEHKKFLEEAKKEGC-C(O)$NH_2$.

(8) The 54-residue HLH peptide was synthesized using Fmoc solid-phase synthesis on a Millipore 9050Plus peptide synthesizer. A PAL PEG-PS resin was utilized; activation was achieved using DIPEA/HOBt. Side-chain deprotection and cleavage from the resin was performed using TFA/phenol/ triisopropylsilane/water (88:5:2:5 v/v). The peptide was purified by reverse phase HPLC, and the molecular weight was confirmed by MALDI-TOF MS. The homodimer protein, $[HLH]_2$ was obtained by air oxidation at pH 8.8. Formation of the dimer was confirmed by gel filtration (see Supporting Information) and MALDI-TOF MS.

(9) $Ru[HLH]_2$ was incubated in 70% TFA for 24 h with a 200-fold molar excess of CNBr. The MALDI-TOF MS spectrum of the digest has a major peak at $m/z = 3767.6$, corresponding to $[(1-28)\text{-}Ru(bpy)_2]^{2+}$ in which a $[1-28\text{-}H]^+$ fragment is cleaved (presumably during the laser ionization process). Together with spectroscopic evidence, this shows that Ru is bound, as designed, to the His21 pairs and not His42.

(10) The 490 nm, 10 ns pulse width output of an optical parametric oscillator pumped at 355 nm was used as the excitation, and a PMT was employed for detection of emission at 645 nm. A 100 $\mu$M $Ru[HLH]_2$ in a $1 \times 1$ cm cuvette was degassed by a series of freeze−pump−thaw cycles.

(11) Luo, J.; Wishart, J. F.; Isied, S. S. *J. Am. Chem. Soc.* **1998**, *120*, 12970.

(12) The 532 nm, 10 ns, 100 mJ output of a pulsed Nd:YAG laser was used for excitation. The probe light (Xe-flashlamp) was passed through a monochromator and detected with a PMT. The kinetics was monitored at 428 nm and averaged over 256 shots. The protein (50 $\mu$M aRC) was thoroughly degassed by a series of freeze−pump−thaw cycles.

(13) Fom the measured redox potentials and the excited energy of bound-Ru (2.1 eV), the driving forces for the forward and back ET, are −0.8 and −1.3 eV, respectively. It is therefore predicted that the forward reaction is nearly activationless, while the back reaction is in the Marcus inverted region. Farid, R. S.; Moser, C. C.; Dutton, P. L. *Curr. Opin. Struct. Biol.* **1993**, *3*, 225−233.

(14) The redox potentials of cyt *c* and naphthoquinone-2-sulfonate are 250 mV and −60 mV, respectively. Therefore, the driving force for reduction of $Ru^{III}$ by reduced cyt *c* is −0.055 eV, and that of oxidation of heme by naphthoquinone-2-sulfonate is −0.95 eV. Given the CSS lifetime of 70 ns, even at 20 $\mu$M of cyt *c* and the quinone, the interception efficiency of the CSS, assuming a diffusion-controlled rate, would be in the range of ~1%.

(15) (a) Kozlov, G. V.; Ogawa, M. Y. *J. Am. Chem. Soc.* **1997**, *119*, 8377. (b) Jones, G., II; Vullev, V.; Braswell, E. H.; Zhu, D. *J. Am. Chem. Soc.* **2000**, *122*, 388. (c) Jones, G., II; Vullev, V. I. *Org. Lett.* **2002**, *4*, 4001.

JA0292142